# Preprints.org

Article

# The Shrinking Fermi Liquid Scenario for Strange-Metal Behavior from Overdamped Optical Phonons

Giovanni Mirarchi , Marco Grilli --- [*] , Goetz Seibold , Sergio Caprara

*Article*

# The Shrinking Fermi Liquid Scenario for Strange-Metal Behavior from Overdamped Optical Phonons

**Giovanni Mirarchi** [1] (ID)**, Marco Grilli** [1,2,*] (ID)**, Götz Seibold** [3] (ID) **and Sergio Caprara** [1,2] (ID)

[1] Dipartimento di Fisica, Università di Roma "La Sapienza", P.le Aldo Moro 5, I-00185 Roma, Italy
[2] CNR-ISC, via dei Taurini 19, I-00185 Roma, Italy
[3] Institut für Physik, BTU Cottbus-Senftenberg - PBox 101344, D-03013 Cottbus, Germany
[*] Correspondence: marco.grilli@roma1.infn.it

**Abstract:** We discuss how the interaction of electrons with an overdamped optical phonon can give rise to a strange-metal behavior over extended temperature and frequency ranges. Although the mode has a finite frequency, an increasing damping shifts spectral weight to progressively lower energies so that, despite the ultimate Fermi liquid character of the system at the lowest temperatures and frequencies, the transport and optical properties of the electron system mimic a marginal Fermi liquid behavior. Within this shrinking Fermi liquid scenario, we extensively investigate the electron self-energy in all frequency and temperature ranges, emphasizing similarities and differences with respect to the marginal Fermi liquid scenario.

**Keywords:** strange-metal behavior; marginal Fermi liquid; high-temperature cuprate superconductors

## 1. Introduction

Despite the long-standing success of Landau's Fermi liquid theory, during the last few decades an increasing number of violations of this paradigm has been observed. One of the most noticeable cases is that of high-temperature cuprate superconductors, where many physical quantities like resistivity [1–4], optical conductivity [5,6], or specific heat [7] display an anomalous behavior in the metallic state either above the superconducting dome in the temperature vs. doping phase diagram, or even below it, when superconductivity is suppressed by strong magnetic fields [8]. The attempt to explain these anomalous behaviors led to the formulation of the so-called *marginal Fermi liquid* (MFL) theory [9,10]. This theory is based on the phenomenological assumption that (a) the electrons interact via a momentum-independent effective interaction with a spectral density $P(\omega)$ and (b) that the latter is flat over a sufficiently large frequency range. The form of the spectral density can be taken as $\mathrm{Im}\, P(\omega) = \lambda \min(\omega, k_B T)$, where $k_B$ is the Boltzmann constant, we take the reduced Planck constant $\hbar = 1$, and $\lambda$ is an effective dimensionless coupling, up to a suitable high-energy cutoff $\omega_0$. In turn, this interaction gives rise to a momentum-independent electron self-energy with an imaginary part of the form $\mathrm{Im}\, \Sigma(\omega) = -\lambda \max(\omega, k_B T)$ or, more physically smoothed, $\mathrm{Im}\, \Sigma(\omega) = -\lambda \sqrt{\omega^2 + (k_B T)^2}$. The corresponding real part of the self-energy then gives rise to a quasiparticle weight vanishing as $Z \sim 1/\log(\omega_0/k_B T)$ for $T \to 0^+$. Within a MFL description, it is possible to correctly reproduce many of the anomalous experimental features [9,10], including the linear-in-$T$ resistivity and the apparent logarithmic divergence of the electronic specific heat at a particular doping level.

Generically, there are two sufficient ingredients to reproduce the linear-in-$T$ resistivity typical of strange metals: a low-energy scattering mechanism extending to low frequencies (smaller than $k_B T$), and a near isotropy of the scattering [11]. Clearly, both these features are provided by the MFL paradigm. Recently, thanks to resonant inelastic X-ray scattering (RIXS) experiments performed on several cuprate compounds, it was possible to identify new charge density collective modes, for a recent review see Ref. [12]. While these modes coexist with the well-known charge density waves

previously predicted [13,14] and observed in the underdoped regime, they are also present in a much wider region of the phase diagram [15], extending to high temperatures and dopings. These collective modes, known as *charge density fluctuations* (CDF), are characterized by a finite but rather small characteristic energy scale $M$ and a quite small (1−2 wavelengths) correlation length, so that their spectral weight is extended over a broad range in momentum space [15,16]. The widespread presence of CDF in the phase diagram, their relatively small characteristic energy scale, and their weak momentum dependence triggered the proposal that CDF provide the scattering mechanism at the origin of the strange-metal properties of cuprates [17,18]. In particular, the two main characteristics that made CDF suitable for this description are the weak momentum dependence, which allows them to mediate a scattering that is essentially isotropic on the Fermi surface (including umklapp processes required to degrade momentum, as required to have non-vanishing conductivity at finite frequencies), and the strong Landau damping, which allows them to reduce their characteristic energy scale while leaving their correlation length unchanged [17,18]. By phenomenologically assuming that the damping, as described by a dimensionless parameter $\gamma$, increases logarithmically with lowering the temperature, in a more or less restricted doping range, a good deal of the strange-metal phenomenology of cuprates was then accounted for.

All the above obviously motivates an analysis of electrons interacting through a dispersionless optical phonon with a substantial Landau damping due to its Holstein-like coupling to the local electron density. The model we are going to propose always exhibits a standard Fermi liquid behavior at low enough temperature, but the range of validity of the Fermi liquid regime shrinks when the Landau damping $\gamma$ is *assumed* to increase with decreasing temperature. Henceforth, we will refer to this model as a shrinking Fermi liquid (SFL). As we shall see, this model displays features both of standard Fermi liquid and of MFL systems, and it could be suitable for the description of some of the most prominent hallmarks of strange metals.

## 2. Self-Energy from a simple local propagator

We consider the retarded propagator of a local (i.e., momentum independent) overdamped collective mode

$$\mathcal{D}_R(\omega) = \frac{1}{M - \mathrm{i}\gamma\omega - \frac{\omega^2}{\Omega}}, \qquad \operatorname{Im}\mathcal{D}_R(\omega) = \frac{1}{\gamma}\frac{\omega}{\left(\dfrac{M}{\gamma} - \dfrac{\omega^2}{\gamma\Omega}\right)^2 + \omega^2}. \tag{1}$$

Since we are going to describe a massive (non-critical) collective mode, we consider $M$ as a fixed parameter of our theory. The generic expression for the imaginary part of a self-energy due to the above collective mode within the Fock approximation is given by [19,20]:

$$\begin{aligned}
\operatorname{Im}\Sigma_R(\omega, T) &= -g^2 \int_{-\infty}^{+\infty} \operatorname{Im}\mathcal{D}(\xi - \omega)\big[f(\xi) + b(\xi - \omega)\big] N(\xi)\,\mathrm{d}\xi \\
&= -\frac{g^2 N_0}{2\gamma} \cosh\!\left(\frac{\beta\omega}{2}\right) \int_{-\infty}^{\infty} \frac{\xi - \omega}{\left[\dfrac{M}{\gamma} - \dfrac{(\xi - \omega)^2}{\gamma\Omega}\right]^2 + (\xi - \omega)^2} \\
&\quad \times \frac{1}{\cosh\!\left(\dfrac{\beta\xi}{2}\right)\sinh\!\left(\dfrac{\beta(\xi - \omega)}{2}\right)}\,\mathrm{d}\xi,
\end{aligned} \tag{2}$$

where $g$ is the coupling between the electrons and the collective mode, $f(\omega)$ and $b(\omega)$ are the Fermi and the Bose functions, respectively. We also assumed a nearly constant density of states $N(\xi) \approx N_0$. A word is in order here about the high frequency behavior of this expression. If we consider an infinite electron bandwidth and an infinite collective mode high-energy scale $\Omega$, $\operatorname{Im}\Sigma_R(\omega, T) \sim \log\omega$ for $\omega \to \infty$. This behavior changes when $\Omega$ is finite, because $\operatorname{Im}\Sigma_R(\omega, T) \to$ constant at large $\omega$, thereby

reproducing the standard behavior of Holstein phonons [21], as the damped character of our collective mode becomes immaterial at frequencies much larger than its characteristic energy scales. On the other hand, as soon as a finite fermion bandwidth is considered, $\text{Im}\,\Sigma_R(\omega, T) \to 0$ at high frequencies, since the phase space for the scattered electrons is reduced. This high-energy effect of a finite bandwidth can be mimicked by introducing an ultraviolet cutoff in the integral of Eq. (2), which must be comparable with the bandwidth itself (this is of order of magnitude of a few hundred meV in cuprates). For the sake of clarity, and to keep the number of parameters in the theory as small as possible, we shall take this high-energy cutoff as infinity.

Eq. (2) can be taken as the starting point for the deduction of all quantitative aspects of our model. Unfortunately, the integral which appears in this expression cannot be analytically solved for any frequency and temperature. However, not only it is quite simple to obtain numerically the self-energy in the general cases, but it is quite instructive and physically interesting to investigate suitably restricted physical regimes.

*2.1. Zero frequency*

We first explore the temperature dependence of the self-energy at fixed $\omega = 0$:

$$\text{Im}\,\Sigma_R(\omega = 0, T) = -\lambda \frac{M}{\gamma} \int_{-\infty}^{+\infty} \frac{\xi}{\left(\dfrac{M}{\gamma} - \dfrac{\xi^2}{\gamma\Omega}\right)^2 + \xi^2} \frac{1}{\sinh(\beta\xi)}\, d\xi.$$

This integral cannot be evaluated analytically, but it is possible to separately consider the two regimes in which the temperature is, respectively, smaller or larger than $M/\gamma$:

$$\text{Im}\,\Sigma_R(\omega = 0, T) \simeq -\pi^2 \lambda \frac{M}{2\gamma}\left(\frac{\gamma k_B T}{M}\right)^2, \qquad \text{for} \quad k_B T \ll M/\gamma,$$

$$\text{Im}\,\Sigma_R(\omega = 0, T) \simeq -\pi \lambda k_B T, \qquad \text{for} \quad k_B T \gg M/\gamma, \tag{3}$$

where $\lambda := g^2 N_0 / M$ is a dimensionless coupling constant. For instance, it was shown in Ref. [16] that $\lambda \approx 0.3 - 0.5$ in the case of slightly overdoped cuprates and, since this is a quite moderate value, the perturbative approach does not seem unreasonable at least in that case. It is most remarkable that $\text{Im}\,\Sigma_R(\omega = 0, T)$ displays a crossover between a quadratic (i.e., Fermi liquid like) and a linear (i.e., of the MFL form) regime around a temperature scale of the order of $M/\gamma$, [see Figure 1]. It is important to notice that the linear-in-$T$ behavior has a quite simple physical explanation: when the temperature becomes of the order of, or larger than, the intrinsic energy scale $M/\gamma$ of the collective modes, these acquire a (nearly) classical statistical weight with the Bose function becoming $\sim k_B T/\omega$. Therefore, the linear-in-$T$ behavior of the resistivity simply arises from this linear statistical dependence on $T$. The same commonly occurs in standard (not overdamped) electron-phonon systems when the temperature is above the Bloch-Grüneisen regime $k_B T \simeq \omega_D/5$ (where $\omega_D$ is the Debye frequency).

Also notice that the slope of the linear regime does not depend on $\gamma$. As it will be discussed in the last section, this feature is particularly interesting in the light of a possible explanation of the linear-in-$T$ resistivity in strange metals, when the superconducting critical temperature is lowered by magnetic fields, thereby extending the linear-in-$T$ regime of the resistivity down to lower and lower temperatures.
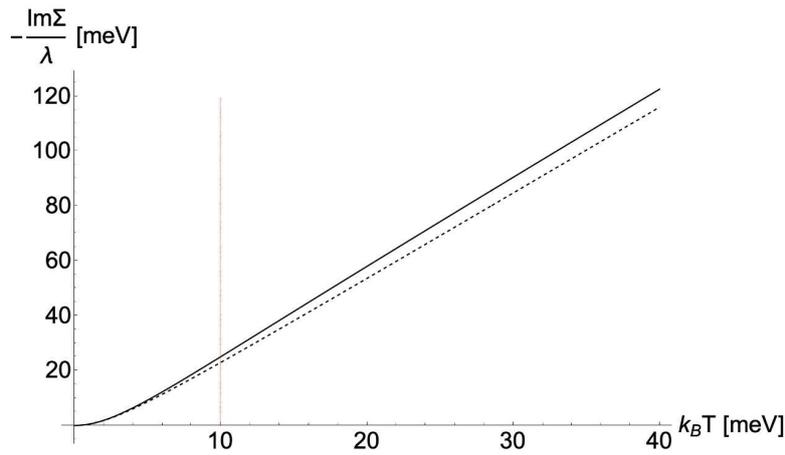
**Figure 1.** Temperature dependence at $\omega = 0$ of the exact [Eq. (2) solid line] and of the approximate form Eq. (8) (dotted line). The vertical red line indicates the crossover temperature from Fermi liquid to linear-in-$T$ regime. Values of the parameters are $M = 10$ meV, $\gamma = 1$, $\Omega = 30$ meV.

## 2.2. Zero temperature

According to Eq. (2), the zero temperature expression for the self-energy is given by

$$\operatorname{Im} \Sigma_R(\omega, T = 0) = -\lambda \frac{M}{2\gamma} \log \left[ 1 + \left( \frac{\gamma\omega}{M} \right)^2 \right],\tag{4}$$

which, for selected parameters, is plotted in Figure 2 by the solid grey line. This expression is obtained in the simpler case of $\Omega \to \infty$, whereas the expression becomes more involved when $\Omega$ is finite,

$$\operatorname{Im} \Sigma_R(\omega, T = 0) = -\frac{\lambda}{2} \frac{M}{\gamma} \int_0^{\omega^2} \frac{1}{\left( \dfrac{M}{\gamma} - \dfrac{x}{\gamma\Omega} \right)^2 + x} \, dx,$$

and the corresponding result is shown by the solid black curve in Figure 2. In the $\Omega \to \infty$ case $\operatorname{Im} \Sigma_R(\omega, T = 0)$ grows logarithmically (of course, until the electron bandwidth is eventually reached), while, when $\omega > \Omega$ and for $\gamma\Omega > 4M/\gamma$, it saturates to a finite value,

$$\operatorname{Im} \Sigma_R(\omega \to \infty, T = 0) = -\lambda \frac{M}{\gamma} \frac{\gamma\Omega}{\sqrt{\gamma^2\Omega^2 - 4M\Omega}} \log \left( \frac{\gamma\Omega + \sqrt{\gamma^2\Omega^2 - 4M\Omega}}{\gamma\Omega - \sqrt{\gamma^2\Omega^2 - 4M\Omega}} \right).\tag{5}$$

Notice that the $\omega \ll M/\gamma$ limit leads to a quadratic dependence in $\omega$, in agreement with a standard Fermi liquid behavior. Due to the constant or weakly divergent behavior at high frequencies, $\operatorname{Im}\Sigma_R(\omega)$ never displays a truly linear-in-$\omega$ behavior, characteristic, e.g., of the MFL state, rather it switches from a quadratic to a logarithmic or constant regime, so that an approximately linear dependence in the crossover region of the inflection point occurs between the two regimes. However, the linear regime is quite extended and for the parameters used in Figure 2 comprises an energy interval of $\sim 15$ meV around the inflection point where the relative difference between exact and linearized $\operatorname{Im}\Sigma_R(\omega)$ is below 5%. One can also notice that the slope of the approximately linear regime of this function does not depend on $\gamma$. This regime is clearly visible around the inflection point of $\operatorname{Im}\Sigma_R(\omega, T = 0)$, which occurs around a frequency

$$\omega_{\text{infl}} = \sqrt{\frac{\sqrt{(\gamma^2\Omega^2 - 2M\Omega)^2 + 12M^2\Omega^2} - (\gamma^2\Omega^2 - 2M\Omega)}{6}}.\tag{6}$$

Notice also that the location of this inflection point, marking the approximately linear regime, depends on the strength of the dissipation parameter $\gamma$. In particular, in the strongly dissipative regime, $\gamma \gg 1$, $\omega_{\text{infl}} \sim M/\gamma$, while in the propagating regime $\gamma \ll 1$, $\omega_{\text{infl}} \sim \sqrt{M\Omega}$.
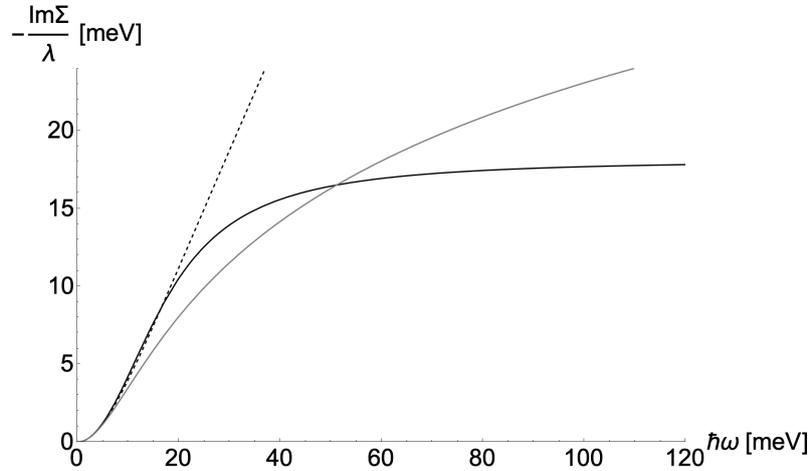


**Figure 2.** Frequency dependence at $T = 0$ of the exact [Eq. (2) solid line] and of the approximate form Eq. (A2) (dotted line). The values of the parameters are $M = 10\,\text{meV}$, $\gamma = 1$, $\Omega = 30\,\text{meV}$. The solid grey curve reports the case with $\Omega = \infty$.

A numerical inspection of $\text{Im}\,\Sigma_R(\omega, T)$ at various temperatures shows that the behavior outlined at $T = 0$ persists up to physically reasonable temperatures.

At fixed $T = 0$, the real part of the self-energy can be exactly computed by means of the Kramers-Kronig relation, obtaining the simpler expression for the $\Omega \to \infty$ case,

$$\text{Re}\,\Sigma(\omega, T = 0) = -\frac{g^2 N_0}{\gamma} \arctan\left(\frac{\gamma\omega}{M}\right).$$

In the case in which $\Omega$ is finite the calculation is considerably more complicated, even when $T = 0$. However, since we are only interested in the quasiparticle weight, we can use the Kramers-Kronig relation to directly calculate the derivative of $\text{Re}\,\Sigma(\omega, T = 0)$ at zero frequency:

$$\frac{\partial \text{Re}\,\Sigma_R(\omega, T = 0)}{\partial \omega}\bigg|_{\omega=0} = \int_0^\infty \frac{1}{\omega}\left[\frac{\partial \text{Im}\,\Sigma_R(\omega', T = 0)}{\partial \omega'}\bigg|_{\omega'=\omega} + \right.$$

$$\left. -\frac{\partial \text{Im}\,\Sigma_R(\omega', T = 0)}{\partial \omega'}\bigg|_{\omega'=-\omega}\right]\frac{\text{d}\omega}{\pi} = -\lambda \int_{-\infty}^\infty \frac{M}{\gamma}\frac{1}{\left(\frac{M}{\gamma} - \frac{\omega^2}{\gamma\Omega}\right)^2 + \omega^2}\frac{\text{d}\omega}{\pi} = -\lambda.$$

Given this result, one can easily compute the quasiparticle weight:

$$Z := \left(1 - \frac{\partial \text{Re}\,\Sigma(\omega, T = 0)}{\partial \omega}\bigg|_{\omega=0}\right)^{-1} = \frac{1}{1+\lambda}. \tag{7}$$

This result shows that the quasiparticle weight at zero temperature is independent of $\gamma$ and that the associated quasiparticle mass enhancement stays finite, $m^*/m = 1 + \lambda$ (obviously the mass parameter of the collective mode, $M$, should not be confused with the quasiparticle mass $m^*$), as long as the dimensionless coupling stays finite. In particular, this would imply that the electron specific heat is not renormalized by $\gamma$ at low temperature, and that the specific heat coefficient $C_V/T$ for the electrons always stays finite (non-critical). This is a consequence of the fact that the low-frequency behavior of $\text{Im}\,\Sigma_R(\omega, T = 0)$ is quadratic in $\omega$, unlike the MFL case, for which we get instead a logarithmically

vanishing quasiparticle weight. As seen in the Appendix A, from the expression at finite $\Omega$, the effect of this ultraviolet cutoff introduces weak $\gamma$-dependent corrections to $Z$ of order $M/(\gamma\Omega)$.

## 3. Discussion and conclusions

### 3.1. The main features of the Overdamped Optical Phonon model

In light of what has been shown so far, we now discuss the most remarkable aspects and physical consequences of the model considered here. First of all, there is a characteristic energy scale $M/\gamma$ that separates the asymptotic regimes both in frequency and in temperature. Below this scale the system is a standard Fermi liquid, which displays the usual $T^2$ and $\omega^2$ behavior of the imaginary part of the fermion self-energy. The quasiparticle mass renormalization at zero temperature only depends on the dimensionless parameter $g^2 N_0/M$ and there is no $\gamma$ dependence.

On the other hand, for $k_B T > M/\gamma$, the system displays a linear-in-$T$ behavior in $\text{Im}\,\Sigma_R$. The same does not hold as far as the frequency dependence is concerned, since the seemingly linear-in-$\omega$ behavior only arises in an extended range around an inflection point in $\text{Im}\,\Sigma_R(\omega)$ separating the $\omega^2$ regime at low frequency and the $\log(\omega)$ or constant regime at high frequency. It is quite important to stress that the different temperature and frequency behaviors stem from completely different physical mechanisms. In contrast to a MFL, where the underlying $\omega$-independent spectral density leads to a linear-in-$\omega$ behavior of $\text{Im}\,\Sigma_R(\omega)$ down to $k_B T$, the frequency dependence in the SFL scenario arises from the dynamical range of the collective mode. This range extends down to low frequency because of the damping and extends up to high frequencies when the overdamped character of the mode persists because of a large $\Omega$, before the collective mode turns into a nearly propagating mode, at $\omega > \Omega$. In passing, we notice the smoother shape of $\text{Im}\,\Sigma_R(\omega)$ in Figure 2 with respect to the usual step-like shape in undamped Einstein phonons [21]. Instead, the truly linear-in-$T$ behavior of $\text{Im}\,\Sigma_R(T)$ arises from the classical statistical weight of the collective modes mediating the quasiparticle scattering. Owing to this different origin, there is no reason to expect any $\omega/T$ scaling in the present model (notice that the other usual mechanism for scaling, namely the divergence of some correlation length near criticality is ineffective here, because the collective modes are massive and non-critical). Nevertheless, as a matter of fact, a seeming scaling *can* be obtained because $\text{Im}\,\Sigma_R(\omega, T)$ can be fitted remarkably well over a sizable temperature and frequency range by an approximate form that is described in detail in Appendix B, and can be further simplified, for the sake of exemplification, in the form

$$\text{Im}\,\Sigma_R(\omega, T) \simeq -\lambda\left[\sqrt{\left(\frac{M}{\gamma}\right)^2 + \omega^2 + (\pi k_B T)^2} - \frac{M}{\gamma}\right]. \tag{8}$$

This expression captures the main features of $\text{Im}\,\Sigma_R(\omega, T)$ at all temperatures and at small/moderate frequencies, and allows to see how our model might display seeming scaling properties over a sizable range, where it not for the presence of a finite mass term $M/\gamma$. It is interesting to note that it may be precisely a mass term $M/\gamma$ of order $10\,\text{meV}$ that accounts for the small scaling violations at low frequencies in optical experiments in slightly overdoped cuprates [6].

Moreover, this expression makes it clear that, for frequencies and temperatures much larger than $M/\gamma$, the imaginary part of the fermion self-energy bears strong similarities with the MFL model, where the fermion self-energy takes the form $\text{Im}\,\Sigma_R(\omega, T) = -\lambda\sqrt{\omega^2 + (k_B T)^2}$.

Eq. (8) also makes it clear that in the linear regimes (both in temperature and in frequency) the slopes are independent of $\gamma$ and $M$. This has an important consequence: for $k_B T, \omega \gg M/\gamma$, an approximate $\omega/T$ scaling is obtained, as it is obvious because in this limit our approximate fitting form, Eq. (8), reduces to the MFL form.

### 3.2. Connection with the Shrinking Fermi Liquid scenario

We now propose a straightforward connection of the presently studied model with the SFL model, as a possible explanation for the strange metallicity of many physical systems. In this regard, we first notice that, since the overdamped optical phonons mediating the inter-particle interaction have no momentum dependence, then the quasiparticle scattering rate coincides with the transport scattering rate. Moreover, owing to the momentum independence of the scattering mechanism, scattering processes obviously include also umklapp processes, responsible for momentum dissipation and non-zero conductivity at finite frequencies. Therefore, the linear regime of $\text{Im}\,\Sigma_R(\omega = 0, T)$ would coincide with a regime of linear-in-$T$ resistivity, which is the most famous and prominent feature of strange metals.

According to our analysis, the linear-in-$T$ behavior stops below a Fermi liquid temperature scale $M/\gamma$. In the strange metals, like, e.g., slightly overdoped superconducting cuprates, this linear resistivity is observed down to the superconducting critical temperature (of order of $10^1 - 10^2\,\text{K}$). This is of the same order of $M/\gamma$, which in cuprates is estimated from RIXS experiments [15,22]. The comparison between the static and dynamical spectral densities of the CDF, allows one to estimate $M$ to be of order $10\,\text{meV}$ and $\gamma$ to be of order one. Therefore, the linear-in-$T$ resistivity would be nicely accounted for by quasiparticles being scattered by CDF (as characterized by RIXS experiments [16]) which, being weakly momentum dependent, are also reasonably well described by the present model. The same occurs as far as the linear-in-$\omega$ behavior is concerned, as schematized by the solid-line curves in Figure 3a, where the (approximate) linear-in-$\omega$ behavior of $\text{Im}\,\Sigma_R(\omega)$ at various fixed temperatures occurs above the $M/\gamma = 10\,\text{meV}$ scale. On the other hand the solid lines at low temperature become substantially different from the dotted lines representing the MFL behavior, which we plot as a benchmark.
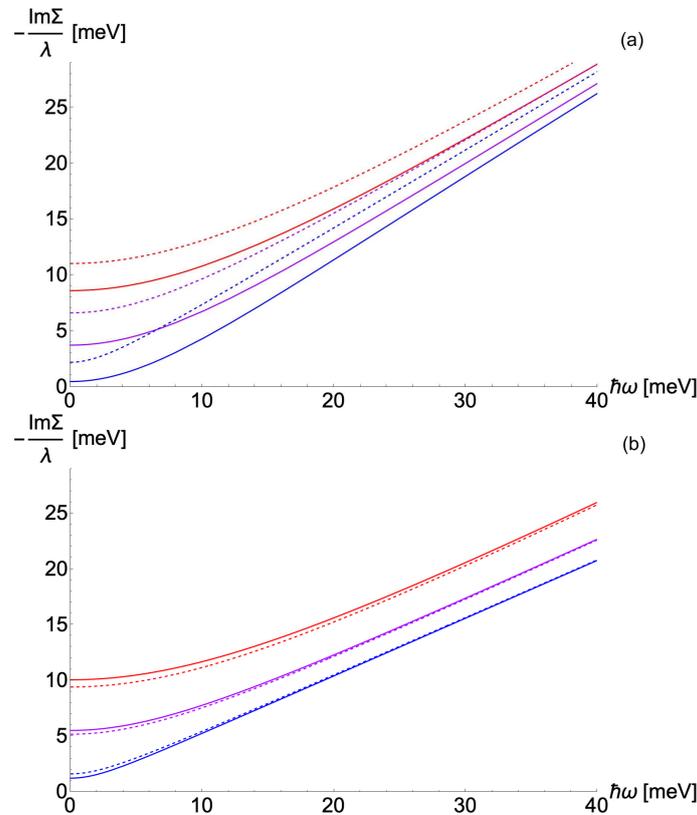


**Figure 3.** Solid lines: Frequency dependence at various temperatures, [$k_\text{B}T = 1\,\text{meV}$ (blue curves), $k_\text{B}T = 3\,\text{meV}$ (magenta curves) and $k_\text{B}T = 5\,\text{meV}$ (red curves)] of the approximate Eq. (A2), in comparison with the MFL expression (dotted lines) at the same temperatures. The values of the parameters are $M = 10\,\text{meV}$, $\gamma = 1$ in (a); $\gamma(T) = \log[20\,\text{mev}/(k_\text{B}T)]$ in (b); $\Omega = 30\,\text{meV}$.

A similar failure arises when the linear-in-$T$ behavior in the d.c. resistivity is shown to persists down to $T \sim 2\,\mathrm{K}$, as found in transport experiments under strong magnetic field [3,8], obviously smaller than $M/\gamma$, *if $\gamma$ does not depend on temperature*. To solve this difficulty, the possibility was considered in Refs. [17,18,20] that $\gamma$ increases with lowering the temperature, when superconductivity is suppressed.

The value of $\gamma$ at low temperatures can be extracted from specific heat experiments. Indeed, it is quite natural that the boson collective modes contribute to the specific heat $C_V$, if their energy is low enough. It is then found [17,18] that the bosonic contribution to $C_V/T$ is proportional to the damping coefficient $\gamma$, and this could in turn be assumed to increase logarithmically in $T$, to match the experimental growth of $C_V/T$ [7]. It is worth emphasizing that, in this scenario, the logarithmic divergence of $C_V/T$ arises from the boson (collective-mode) contribution and not from the fermions, which behave as Fermi liquid quasiparticles, with a finite mass [see Eq. (7)]. While a full microscopic model for this increase is still missing, a simplified model based on the interplay between CDF and diffusion modes of the electrons was also proposed in Ref. [20] for two-dimensional systems, accounting for a logarithmic-in-$T$ increase of $\gamma$, with decreasing $T$. Then, assuming $\gamma(T) = \log[20\,\mathrm{mev}/(k_\mathrm{B}T)]$, the whole Fermi liquid scale $M/\gamma(T)$ *shrinks*, so that the region of Fermi liquid behavior is correspondingly reduced at lower temperatures. This behavior is reported in Figure 3b. Here, it is evident that the Fermi liquid scale $M/\gamma(T)$ shrinks with decreasing $T$, in such a way as to keep the solid lines, reporting the numerical evaluation of $\mathrm{Im}\,\Sigma_R(\omega, T)$, close to the MFL dotted curves even at low temperatures. In order to have a better quantitative comparison between the two scenarios, we chose to use Eq. (A2) [rather than the more schematic Eq. 8] as a fitting expression for $\mathrm{Im}\,\Sigma_R(\omega, T)$. As discussed in Appendix B, this expression shares all the qualitative aspects of Eq. (8) discussed so far, but in addition it also more precisely reproduces the slope of the linear part in $\omega$ at $T = 0$.

One could also wonder whether a $T$-dependent $\gamma$ might alter the linear-in-$T$ behavior of $\mathrm{Im}\,\Sigma_R(\omega = 0, T)$ [hence, of the d.c. resistivity $\rho(T)$]. The fact mentioned above, that the slope of $\mathrm{Im}\,\Sigma_R(\omega = 0, T)$ does not depend on $\gamma$, comes at rescue, by allowing to keep the slope of $\rho(T)$ unchanged while the Fermi liquid scale is progressively reduced at lower and lower temperatures.

Hence, our overdamped optical phonon model, once it is equipped with the additional feature of a $\gamma(T)$ increasing logarithmically with lowering $T$, gives rise to a SFL scenario. By (phenomenologically) assuming this temperature dependence of $\gamma(T)$, to fit the experimentally measured $C_V/T$, this scenario, although ultimately based on a Fermi liquid state at $T = 0$, mimics quite well (and it is, to any practical purpose, indistinguishable from) the MFL behavior, without invoking an unnecessary $\omega/T$ scaling in the boson spectrum.

## Abbreviations

The following abbreviations are used in this manuscript:

MFL    Marginal Fermi Liquid
CDF    Charge Density Fluctuations
SFL    Shrinking Fermi liquid

## Appendix A

In order to find an interpolating expression for our self-energy valid at any frequency and temperature, it is convenient to approximate the Bose and Fermi functions with piecewise polynomial functions, as it is customary:

$$
f(\omega) \simeq
\begin{cases}
1, & \text{for } \omega < -2k_{\mathrm{B}}T, \\
\dfrac{1}{2} - \dfrac{\omega}{4k_{\mathrm{B}}T}, & \text{for } -2k_{\mathrm{B}}T \leq \omega \leq 2k_{\mathrm{B}}T, \\
0, & \text{for } \omega > 2k_{\mathrm{B}}T;
\end{cases}
$$

$$
b(\omega) \simeq
\begin{cases}
-1, & \text{for } \omega < -2k_{\mathrm{B}}T, \\
\dfrac{k_{\mathrm{B}}T}{\omega} - \dfrac{1}{2}, & \text{for } -2k_{\mathrm{B}}T \leq \omega \leq 2k_{\mathrm{B}}T, \\
0, & \text{for } \omega > 2k_{\mathrm{B}}T.
\end{cases}
$$

By using these approximations, and by considering only the case $\Omega \to \infty$, the integral in Eq. (2) becomes fully analytical. Since our approximated forms for $f(\omega)$ and $b(\omega)$ become exact at $T = 0$ we expect to recover Eq. (4) at zero temperature. At $\omega = 0$ this approximation reproduces the correct expression at high temperature but it gives an incorrect expression for a factor $3\pi^2/16$ at low temperature, due to the fact that the integral of $f(\xi) - b(\xi - \omega)$ in $\mathrm{d}\xi$ changes by that factor if the exact or approximate expression is used. By correcting this discrepancy by hand, we obtain the following smoothly interpolating expression for the self-energy:

$$
\operatorname{Im}\Sigma_R(x,y) = -\frac{\alpha}{4} \log\left[ \frac{\left(1 + (x+cy)^2\right)\left(1 + (x-cy)^2\right)}{\left(1 + (cy)^2\right)^2} \right] - 2\alpha y \arctan(cy) +
$$
$$
+ \frac{2\alpha}{c}\left[ 1 - \frac{\arctan(x+cy) - \arctan(x-cy)}{2cy} - \frac{x}{4cy} \log\left( \frac{1 + (x+cy)^2}{1 + (x-cy)^2} \right) \right],
\tag{A1}
$$

where we have introduced the following definitions:

$$
\alpha := \frac{g^2 N_0}{\gamma}, \qquad x := \frac{\gamma\omega}{M}, \qquad y := \frac{\gamma k_{\mathrm{B}}T}{M}, \qquad c := \frac{3\pi^2}{8}.
$$

It is quite straightforward to show that equation (A1) correctly reproduces Eq. (4) and (3) in the appropriate domains of validity. Note that this expression has the form:

$$
\operatorname{Im}\Sigma_R(\omega, T) = -\frac{g^2 N_0}{M} \frac{M}{\gamma} F\left( \frac{\gamma\omega}{M}, \frac{\gamma k_{\mathrm{B}}T}{M} \right),
$$

where the dimensionless positive-definite function $F(\gamma\omega/M, \gamma k_{\mathrm{B}}T/M)$ is fully defined through Eq. (A1). Notice that it is a scaling function separately between $\omega$ and $M/\gamma$ and between $k_{\mathrm{B}}T$ and $M/\gamma$, but not between $\omega$ and $k_{\mathrm{B}}T$. This is another important difference between the standard MFL and our SFL.

## Appendix B

Once the above simplified expressions of $b(\omega)$ and $f(\omega)$ are used, the integral which appears in Eq. ((2)) has an exact expression in terms of elementary functions. However, the full expression does not enlighten the physics behind it. It is instead interesting to observe the behavior of this expression

in appropriate regimes. There are only two energy scales involved in the qualitative behavior of $\mathrm{Im}\,\Sigma_R(\omega, T = 0)$, one of which is the aforementioned $\omega_{\mathrm{infl}}$, while we denote the other by $\omega_{\mathrm{sat}}$. In order to have a more compact description, it is convenient to introduce the dimensionless parameter $\phi := \gamma^2 \Omega / M$. We can therefore express these two energy scales as:

$$\omega_{\mathrm{infl}} := \frac{M}{\gamma} \sqrt{\phi \frac{\sqrt{(\phi - 2)^2 + 12} - (\phi - 2)}{6}}, \qquad \omega_{\mathrm{sat}} := \max\left(\frac{M}{\gamma}\phi, \, \omega_{\mathrm{infl}}\right).$$

Notice that both these scales can be expressed as the product of $M/\gamma$ and a dimensionless function of $\phi$. As we mentioned, the function $\mathrm{Im}\,\Sigma_R(\omega, T = 0)$ goes as $\omega^2$ at small $\omega$ and saturates to a constant value at large $\omega$. The two limiting regimes are connected by an extended inflection region, and the frequency scale $\omega_{\mathrm{infl}}$ is defined precisely as the inflection point. The scale $\omega_{\mathrm{sat}}$ is instead the approximate scale beyond which the saturation regime is observed:

$$\mathrm{Im}\,\Sigma_R(\omega, T = 0) \simeq \begin{cases} -\dfrac{\lambda}{2}\dfrac{M}{\gamma}\left(\dfrac{\gamma\omega}{M}\right)^2, & \text{for } \omega \ll \omega_{\mathrm{infl}}, \\[2ex] -\lambda\dfrac{\Lambda_\phi}{2}\omega, & \text{for } \omega \simeq \omega_{\mathrm{infl}}, \\[2ex] \mathrm{Im}\,\Sigma_R(\omega \to \infty, T = 0), & \text{for } \omega \gg \omega_{\mathrm{sat}}, \end{cases}$$

where $\Lambda_\phi$ is a dimensionless parameter that establishes the correct slope of $\mathrm{Im}\,\Sigma_R(\omega, T = 0)$ at its inflection point and it is defined as

$$\Lambda_\phi = \frac{2\sqrt{\phi \dfrac{\sqrt{(\phi - 2)^2 + 12} - (\phi - 2)}{6}}}{\left(1 - \dfrac{\sqrt{(\phi - 2)^2 + 12} - (\phi - 2)}{6}\right)^2 + \phi \dfrac{\sqrt{(\phi - 2)^2 + 12} - (\phi - 2)}{6}}$$

This is a monotonically decreasing function of $\phi$ which approaches 1 in the limit $\phi \to \infty$ and goes as $2/\sqrt{\phi}$ for $\phi \to 0$. The simplest fitting expression that can preserve the correct features of $\mathrm{Im}\,\Sigma_R(\omega, T = 0)$ for $\omega \leq \omega_{\mathrm{infl}}$ is the following:

$$\begin{cases} \mathrm{Im}\,\Sigma_R(\omega, T = 0) \simeq -\lambda\dfrac{M}{\gamma}\left[\sqrt{1 + \left(\dfrac{4 + \Lambda_\phi^2}{4\Lambda_\phi}\dfrac{\gamma\omega}{M}\right)^2} - \sqrt{1 + \left(\dfrac{4 - \Lambda_\phi^2}{4\Lambda_\phi}\dfrac{\gamma\omega}{M}\right)^2}\right], \\[3ex] 1 \leq \Lambda_\phi \leq 2. \end{cases}$$

Given this expression, it is possible to exhibit an even more general fitting expression that can also take the temperature dependence into account:

$$\mathrm{Im}\,\Sigma_R(\omega, T) \simeq -\lambda\left[\sqrt{\left(\dfrac{M}{\gamma}\right)^2 + \left(\dfrac{4 + \Lambda_\phi^2}{4\Lambda_\phi}\omega\right)^2 + (\pi k_B T)^2} - \sqrt{\left(\dfrac{M}{\gamma}\right)^2 + \left(\dfrac{4 - \Lambda_\phi^2}{4\Lambda_\phi}\omega\right)^2}\right], \quad \text{(A2)}$$

which is only valid under these two constraints:

$$1 \leq \Lambda_\phi \leq 2 \quad \wedge \quad k_B T < \frac{4\Lambda_\phi \sqrt{2(16 + \Lambda_\phi^4)}}{\pi(4 - \Lambda_\phi^2)^2}\frac{M}{\gamma}.$$

The second constraint ensures that the fitting expression we have proposed is always an increasing function of $\omega$, and that its behavior at low $\omega$ is quadratic. For reasonable values of $M$, $\gamma$ and $\Omega$, $\Lambda_\phi$ is quite close to 1, however as long as $1 \leq \Lambda_\phi \leq 2$ holds there are no important qualitative changes in the fitting expression. This expression has all the qualitative features of Eq. (8), in particular the latter is reproduced exactly when $\omega = 0$ or $\Lambda_\phi = 2$.

## References

1. Gurvitch T., Fiory A. T., Resistivity of $La_{1.825}Sr_{0.175}CuO_4$ and $YBa_2Cu_3O_7$ to 1100 K: Absence of saturation and its implications. *Phys. Rev. Lett.* **1987** *59*, 1337

2. Hussey, N. E. Phenomenology of the normal state in-plane transport properties of high-Tc cuprates. *J. Phys.: Condens. Matt.* **2008**, *20*, 123201.

3. Proust, C. and Taillefer, L. P. The remarkable underlying ground states of cuprate superconductors. *Annu. Rev. Conden. Mater*. **2019**, *10*, 409.

4. Varma, C. M. Colloquium: Linear in temperature resistivity and associated mysteries including high temperature superconductivity. *Rev. Mod. Phys.* **2020**, *92*, 031001.

5. van der Marel, D. et al. Quantum critical behaviour in a high-Tc superconductor. *Nature* **2003**, *425*, 271.

6. Michon B. et al. Reconciling scaling of the optical conductivity of cuprate superconductors with Planckian resistivity and specific heat. **2023**, *14*, 3033.

7. Michon B. et al., *Nature* **2019**, *567*, 218.

8. Legros A., et al., Universal *T*-linear resistivity and Planckian dissipation in overdoped cuprates. *Nat. Phys.* **2019**, *15* 142.

9. Varma C. M., Littlewood P. B., Schmitt-Rink S., Abrahams E., Ruckenstein A. E., Phenomenology of the normal state of Cu-O high-temperature superconductors. *Phys. Rev. Lett.* **1989**, *63*, 1996.

10. Littlewood P. B. and Varma C. M., Phenomenology of the superconductive state of a marginal Fermi liquid. *Phys. Rev. B* **1992**, *46*, 405.

11. Hlubina R. and Rice T. M., *Phys. Rev. B* **1995**, *51*, 9253.

12. Arpaia R. and Ghiringhelli G., *Charge Order at High Temperature in Cuprate Superconductors*. *J. Phys. Soc. Japan* **2021**, *90*, 111005.

13. C. Castellani, C. Di Castro, and M. Grilli, Singular Quasiparticle Scattering in the Proximity of Charge Instabilities. *Phys. Rev. Lett.*, *75*, 4650 (1995).

14. S. Andergassen, S. Caprara, C. Di Castro, and M. Grilli, Anomalous Isotopic Effect Near the Charge-Ordering Quantum Criticality. *Phys. Rev. Lett.*, *87*, 056401 (2001).

15. R. Arpaia et al., Dynamical charge density fluctuations pervading the phase diagram of a Cu-based high-Tc superconductor, *Science* **365**, 906-910 (2019)

16. G. Seibold et al., Strange metal behaviour from charge density fluctuations in cuprates, *Comm. Phys.*, **4**, 7, (2021).

17. S. Caprara et al., Dissipation-driven strange metal behavior, *Comm. Phys.*, **5**, 10 (2022)

18. G. Mirarchi et al., The Strange-Metal Behavior of Cuprates, *Condens. Matt.*, **7** (1), 29 (2022)

19. G. Mazza, M. Grilli, C. Di Castro, S. Caprara, Evidence for phonon-like charge and spin fluctuations from an analysis of angle-resolved photoemission spectra of $La_{2-x}Sr_xCuO_4$ superconductors, *Phys. Rev. B*, **87**, 014511 (2013).

20. M. Grilli, et al., Dissipative Quantum Criticality as a Source of Strange Metal Behavior, *Symm.*, **15** (3), 569 (2023).

21. Engelsberg, S. and Schrieffer, J. R., Coupled Electron-Phonon System. *Phys. Rev.* **1963**, *131*, 993.

22. Arpaia, R, et al., Signature of quantum criticality in cuprates by charge density fluctuations, *Nat. Commun.* **2023**, *14*, 7198.